TECHNICAL UNIVERSITY OF CLUJ-NAPOCA

ACTA TECHNICA NAPOCENSIS

Series: Applied Mathematics, Mechanics, and Engineering
Vol. 68, Issue I, March, 2025

COMPARATIVE ANALYSIS OF THE 4-RRRP FOUR-BAR LINKAGE AND THE 7-PR(RRRR)RP SEVEN-BAR LINKAGE FOR THE DESIGN OF A MEDICAL DISINFECTION ROBOT WITH FOLDING MECHANISM

Elida-Gabriela TULCAN, Carmen STICLARU, Melania Olivia SANDU, Erwin-Christian LOVASZ

Abstract: *The symmetrical 7-PR(RRRR)RP seven-bar linkage and the 4-RRRP four-bar linkage are compared in this study to determine which is more feasible for the design and development of a medical disinfection robot with a folding mechanism structure. In order to perform sanitation procedures in the hard-to-reach places from various medical facilities, the optimal solution should allow the greatest variation of the mechanism's total height between folded position (which is considered to be the minimum configuration) and the extended position (which is considered to be the maximum configuration), while simultaneously maintaining the robot's size as small as possible.*
Key words: *service robots, disinfection robots, four-bar linkages, seven-bar linkages, folding mechanisms*

1. INTRODUCTION

The employment of medical disinfection robots to carry out disinfection in various settings is growing these days [1]. They use many different kinds of technologies, each with unique benefits and drawbacks [2].

Pulsed xenon UV lamps [3] or mercury-vapor UV lamps [4] are the most common disinfection sources. Nevertheless, in some situations, chlorine compounds [5] or dry mist hydrogen peroxide [6] may also be used for the sanitation processes. Incorporating both UV-C and disinfectant spraying technology allows for the best of both worlds [7].

This work is one of several [8,9] that analyzes and compares various planar mechanisms to identify the most suitable linkage for the development of a medical robot with a folding mechanism used for sanitation procedures.

These kinds of linkages are taken into consideration since they offer a significant height difference of the mechanism between its two extreme positions, therefore facilitating the disinfection of both the difficult-to-reach places and other kinds of areas from multiple locations.

Large settings and places that are hard to reach cannot be disinfected by medical disinfection robots which are only capable of operating in one configuration, as has already been shown [10]. Therefore, to increase the overall efficacy of disinfection procedures, robots with a folding mechanism structure should be further considered.

2. THE FOUR-BAR LINKAGE

Fig. 1 presents the kinematic design of the considered 4-RRRP four-bar linkage. In this notation R stands for revolute joint, P for prismatic joint, while underlined is the drive joint.

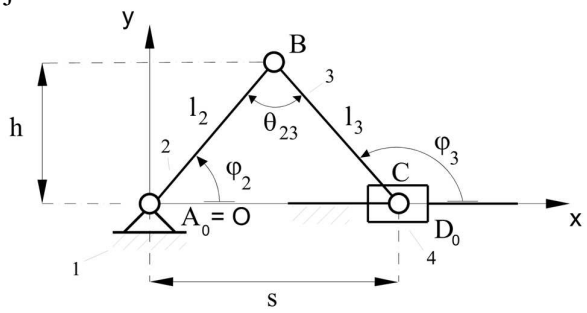

Fig. 1. Kinematic design of the four-bar linkage

The symbol s represents the mechanism's stroke, h represents the height, l_2 and l_3 represent the lengths of the elements, φ_2 and φ_3 represent the positional angles, while θ_{23} represents the input transmission angle.

The folding mechanism has two extreme configurations:

• minimum configuration (folded position), where the values of φ_2 and h are minimum, whereas the values of φ_3, s and θ_{23} are maximum.

• maximum configuration (extended position), where the values of φ_3, s and θ_{23} are minimum, whereas the values of φ_2 and h are maximum.

The vectorial equation, which describes the four-bar linkage, is:

$$s = l_2 \cdot e^{i\cdot\varphi_2} - l_3 \cdot e^{i\cdot\varphi_3} \qquad (1)$$

from which it results:

$$\varphi_2(s) = arccos\left(\frac{s^2 + {l_2}^2 - {l_3}^2}{2 \cdot s \cdot l_2}\right) \qquad (2)$$

$$\varphi_3(s) = arccos\left(\frac{-s^2 + {l_2}^2 - {l_3}^2}{2 \cdot s \cdot l_3}\right) \qquad (3)$$

Furthermore, the height of the mechanism results from the next equation:

$$h(s) = \frac{2 \cdot \sqrt{p(s) \cdot (p(s) - l_2) \cdot (p(s) - l_3) \cdot (p(s) - s)}}{s} \qquad (4)$$

where the semiperimeter $p(s)$ is expressed as:

$$p(s) = \frac{s + l_2 + l_3}{2} \qquad (5)$$

The input design values of the four-bar linkage were chosen due to functional requirements as follows:

- lengths of elements l_2 and $l_3$were chosen to be identical ($l_2 = l_3 = 300$ mm).
- input transmission angle (θ_{23}) takes values between 30° in the extended position and 120° in the folded position.

The positional angles φ_2 and φ_3 as a function of stroke s are shown graphically in Fig. 2 and Fig. 3. According to the representation, angle φ_2 values decrease as stroke s values increase, whereas angle φ_3 values rise simultaneously with stroke s values.

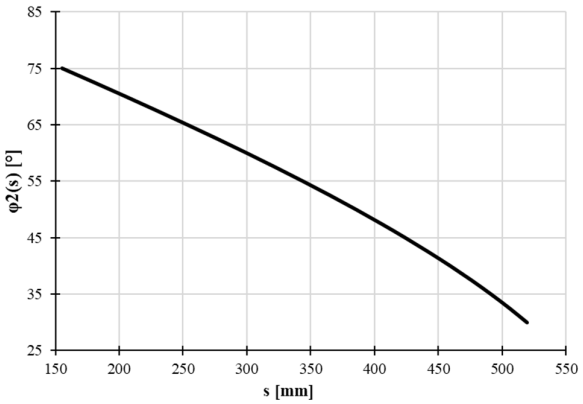

Fig. 2. Graphical representation of $\varphi_2(s)$

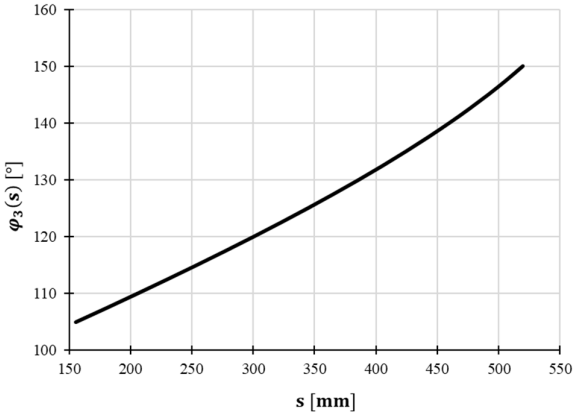

Fig. 3. Graphical representation of $\varphi_3(s)$

Furthermore, a visual representation of height h as a function of stroke s is shown in Fig. 4. As it is seen, the values of stroke s increase while the values of height h decrease.

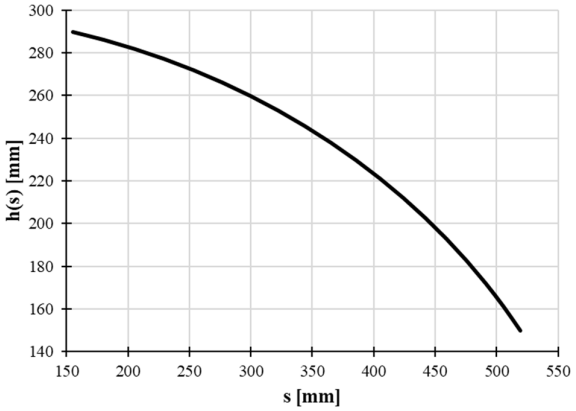

Fig. 4. Graphical representation of h(s)

Table 1 presents the design parameters' values of the 4-RRRP four-bar linkage in the folded position.

The purpose of this configuration is to disinfect the areas with limited space from the medical environment, like the regions beneath the hospital bed and other furnishings, that are known to be full of different types of bacteria and viruses. In addition, since the total stroke of the linkage s_{max} is almost 520 mm, this configuration is also feasible for the floor disinfection, since it can disinfect a large region simultaneously, and thus it helps improve the overall disinfection process effectiveness.

Table 1

Design parameters' values in the folded position

Parameter	Value
$\varphi_{2_{min}}$	30 °
$\varphi_{3_{max}}$	150 °
$\theta_{23_{max}}$	120 °
h_{min}	150 mm
s_{max}	519,6 mm

Table 2 presents the design parameters' values of the 4-RRRP four-bar linkage in the extended position.

Table 2

Design parameters' values in the extended position

Parameter	Value
$\varphi_{2_{max}}$	75 °
$\varphi_{3_{min}}$	105 °
$\theta_{23_{min}}$	30 °
h_{max}	289,7 mm
s_{min}	155,2 mm

3. THE SEVEN-BAR LINKAGE

Fig. 5 shows the kinematic design of the considered symmetrical 7-PR(RRRR)RP seven-bar linkage.

The lengths of the driven elements, l_4 and l_5, as well as the lengths of the drive elements, l_3 (which is $l_{31} + l_{32}$) and l_6 (which is $l_{61} + l_{62}$), were selected to be identical according to design and functional considerations.

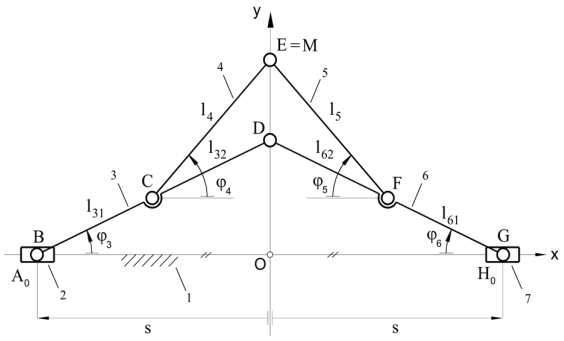

Fig. 5. Kinematic design of the seven-bar linkage

The vectorial equation which describes the seven-bar linkage is:

$$-s + l_{31} \cdot e^{i \cdot \varphi_3} + l_4 \cdot e^{i \cdot \varphi_4} = i \cdot y_M \qquad (6)$$

while the positional angles φ_3 (which is equal to φ_6) and φ_4 (which is equal to φ_5) can be expressed as it follows:

$$\varphi_3(s) = \arccos\left(\frac{s}{l_{31}+l_{32}}\right) \qquad (7)$$

$$\varphi_4(s) = \arccos\frac{l_{32} \cdot s}{l_4 \cdot (l_{31}+l_{32})} \qquad (8)$$

The input design values of the symmetrical seven-bar linkage were chosen due to functional requirements as follows:

- the stroke *s* is ranging between 50 mm in the minimum configuration (folded position) and $(l_{31} + l_{32} - 10)$ mm in the maximum configuration (extended position).
- $l_{31} = l_{32} = l_{61} = l_{62} = 120$ mm.
- $l_4 = l_5 = 170$ mm.

Fig. 6 and Fig. 7 illustrate the graphical representation of the positional angles φ_3 and φ_4 as a function of the stroke *s*. As it is shown, both the values of the angles φ_3 and φ_4 increase together with the values of stroke *s*.

Moreover, the values of the design parameters in the folded and extended positions of the seven-bar linkage are shown in Table 3 and Table 4.

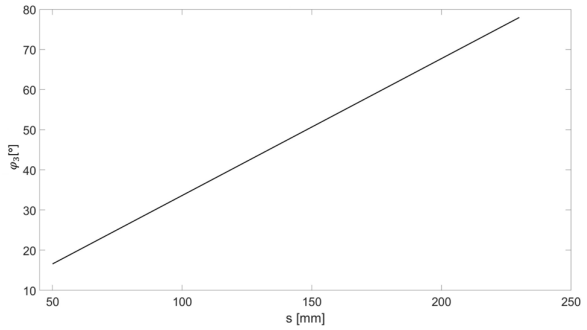

Fig. 6. Graphical representation of $\varphi_3(s)$

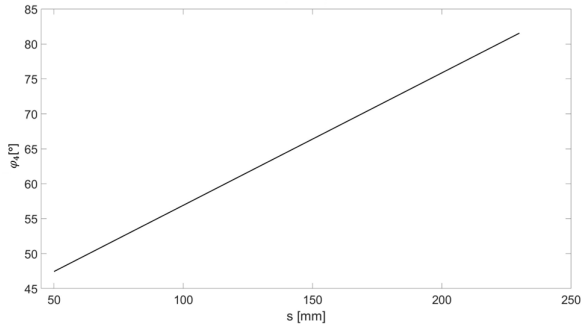

Fig. 7. Graphical representation of $\varphi_4(s)$

Table 3

Design parameters' values in the folded position

Parameter	Value
$\varphi_{3\min} = \varphi_{6\min}$	16,5°
$\varphi_{4\min} = \varphi_{5\min}$	47,4°
s_{max}	230 mm
h_{min}	159 mm

Table 4

Design parameters' values in the extended position

Parameter	Value
$\varphi_{3max} = \varphi_{6max}$	77,9°
$\varphi_{4max} = \varphi_{5max}$	81,5°
s_{min}	50 mm
h_{max}	285 mm

The seven-bar linkage's minimal and maximum configurations are shown in Fig. 8.

4. COMPARATIVE ANALYSIS

When it comes to the presented linkages, both are similar considering they are folding mechanisms which allow two extreme configurations, the folded and the extended position.

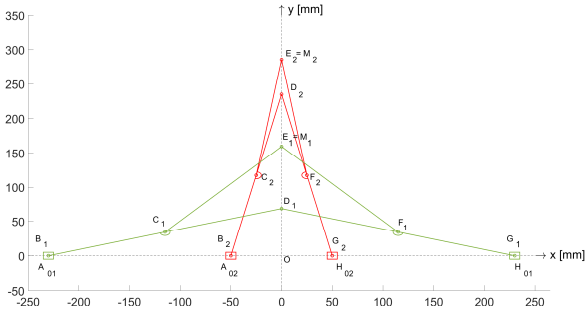

Fig. 8. The seven-bar linkage's folded position (green) and extended position (red)

Therefore, the results of both mechanisms will be analyzed in the minimum and maximum configuration, in order to establish the comparison winner.

4.1. Folded Position

For a better analysis, the resulting parameters of the 4-RRRP four-bar linkage and the symmetrical 7-PR(RRRR)RP seven-bar linkage in the folded position are presented in Table 5.

Table 5

The values of the four-bar and seven-bar linkages' design parameters in the folded position

Parameter	Four-bar linkage Value	Seven-bar linkage Value
Positional angle 1	30°	16,5°
Positional angle 2	150°	132,6°
Output transmission angle	120 °	85,1°
Total stroke	519,6 mm	460 mm
Total height	150 mm	159 mm

Fig. 9 illustrates the analyzed mechanisms in their minimum configuration, the folded position.

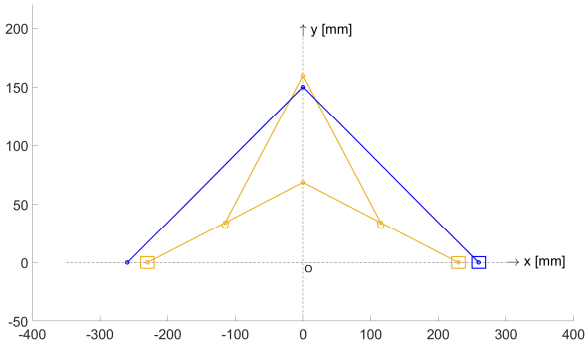

Fig. 9 The four-bar linkage's folded position (blue) and extended position (orange)

As can be seen, the total height of the seven-bar mechanism is slightly greater than the four-bar mechanism's height.

Nevertheless, the total stroke difference between the two mechanisms is quite big, which means that the size of the four-bar linkage will be significantly greater than the seven-bar linkage's size. This is considered to be a disadvantage given that the medical disinfection robot's scope is to be able to disinfect the difficult-to-access areas of the medical institutions, where space is typically limited and restricted.

4.2. Extended Position

Likewise, for a better analysis, the resulting parameters of the 4-RRRP four-bar linkage and the symmetrical 7-PR(RRRR)RP seven-bar linkage in the extended position are presented in Table 6.

Table 6

The values of the four-bar and seven-bar linkages' design parameters in the extended position

Parameter	Four-bar linkage Value	Seven-bar linkage Value
Positional angle 1	75 °	77,9°
Positional angle 2	105 °	98,5°
Output transmission angle	30 °	17 °
Total stroke	155,2 mm	100 mm
Total height	289,7 mm	285 mm

Fig. 10 illustrates the analyzed mechanisms, the four-bar linkage and the seven-bar linkage in their minimum configuration, the folded position.

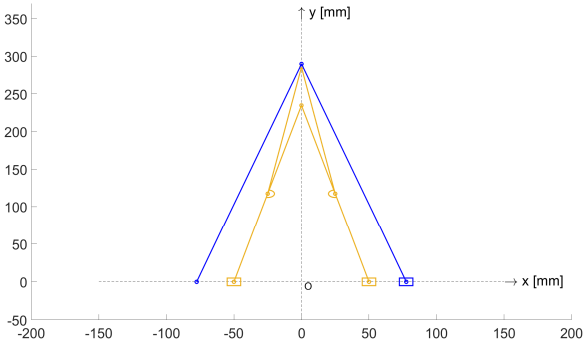

Fig. 10 Extended position of the four-bar linkage (blue) and the seven-bar linkage (orange)

As can be noticed, the symmetrical seven-bar linkage's overall height in the extended position is slightly greater compared to the height of the four-bar linkage.

Nevertheless, the total stroke of the four-bar linkage is again greater than the seven-bar linkage's stroke. It is also true that in this configuration the size of the mechanism does not count as much as in the minimum configuration, but the height difference of not even 5 mm between the two linkages does not justify considering the four-bar linkage more feasible than the seven-bar linkage, since its size still remains a disadvantage when it operates in the folded position.

5. CONCLUSIONS

The paper presented a comparative analysis of the 4-RRRP four-bar linkage and the symmetrical 7-PR(RRRR)RP seven-bar linkage.

Since it offers the best balance between the height difference between the minimum and maximum configuration and the overall size, the symmetrical 7-PR(RRRR)RP seven-bar linkage is a more feasible structure for the design of a disinfection robot with folding mechanism than the 4-RRRP four-bar linkage, as can also be found throughout the chapters of this paper.

6. REFERENCES

[1] Mehta I., Hsueh H.-Y., Taghipour S., Li W., Saeedi S., *UV Disinfection Robots: A Review*, Robotics and Autonomous Systems, 161, 104332, 2023.

[2] Diab-El Schahawi M., Zingg W., Vos M., Humphreys H., Lopez-Cerero L., Fueszl A., Zahar J.R., Presterl E., *Ultraviolet disinfection robots to improve hospital cleaning: Real promise or just a gimmick?*, Antimicrobial Resistance & Infection Control 10(33), 2021.

[3] Jinadatha C., Quezada R., Huber T., Williams J., Zeber J. and Copeland L., *Evaluation of a pulsed-xenon ultraviolet room disinfection device for impact on contamination levels of methicillin-resistant Staphylococcus aureus*, BMC Infectious Diseases (14), 187, 2014.

[4] McGinn C., Scott R., Donnelly N., Roberts K., Bogue M., Kiernan C. and Beckett M., *Exploring the applicability of robot assisted UV disinfection in radiology*, Frontiers in Robotics and AI (7), 2021.

[5] Zhao Y., Huang H., Chen T., Chiang P., Chen Y., Yeh J., Huang C., Lin J. and Weng W., *A Smart Sterilization Robot System with Chlorine Dioxide for Spray Disinfection*, IEEE Sensors Journal 21(19), pp. 22047–22057, 2021.

[6] Ruan K., Wu Z., Xu Q., *Smart Cleaner: A New Autonomous Indoor Disinfection Robot for Combating the COVID-19 Pandemic*, Robotics 10(3), 2021.

[7] Van T. N., Xuan N.H. and Duc N.N., *Design and development of multifunctional autonomous mobile disinfection robot against SARS-CoV-2 virus*, International Journal of Mechanical Engineering and Robotics Research 11(10), pp. 718-723, 2022.

[8] Tulcan, E.-G., Sticlaru, C., Lovasz, E.-C., *Design of a Medical Robot with Folding Mechanism Used for Disinfection in the Hard-to-Reach Areas*, In: "New Trends in Medical and Service Robotics", Mechanisms and Machine Science, 133, pp. 351–359, Craiova, May, 2023, Springer, Cham.

[9] Tulcan, E.-G., Sticlaru, C., Oarcea, A., Sandu M.O., Lovasz, E.-C., *Kinematic Analysis of the Seven-Bar Linkage 7-PR(RRRR)RP Used for Medical Disinfection Robot*, In: "Advances in Service and Industrial Robotics", Mechanisms and Machine Science, 157, pp. 359–367, Cluj-Napoca, May, 2024, Springer, Cham.

[10] Tulcan E.-G., Sticlaru C., Oarcea A. and Lovasz E.-C., *Medical Disinfection Robots: Past vs Future. Improving the Disinfection Process by Using Disinfection Robots with Folding Mechanism*, 17th International Conference on Engineering of Modern Electric Systems (EMES), pp. 1-4, Oradea, July, 2023, IEEE.

Analiză comparativa între un mecanism cu patru elemente și un mecanism cu șapte elemente

Lucrarea prezintă o analiză comparativă între mecanismul cu patru elemente 4-RRRP și mecanismul cu șapte elemente 7-PR(RRRR)RP pentru a concluziona care dintre aceste variante este mai fezabilă în vederea proiectării unui robot medical de dezinfecție cu mecanism de pliere. Cea mai bună opțiune ar trebui să permită cea mai mare variație a înălțimii mecanismului între configurația minimă (poziția pliată) și configurația maximă (poziția extinsă), păstrând în același timp dimensiunea robotului cât mai mica posibilă, pentru a se putea efectua procesul de dezinfecție în zonele greu accesibile din instituțiile medicale.

Cuvinte cheie: *roboți de service, roboți de dezinfecție, legături cu patru bare, legături cu șapte bare, mecanisme de pliere*

Elida-Gabriela TULCAN, PhD Candidate, Assistant Professor, Politehnica University of Timișoara, Department of Mechatronics, elida.tulcan@upt.ro, +40256403559, Mihai Viteazul Bd., no. 12, Timișoara.

Carmen STICLARU, Dr. ing., Associate Professor, Politehnica University of Timișoara, Department of Mechatronics, carmen.sticlaru@upt.ro, +40256403559, Mihai Viteazul Bd., no. 12, Timișoara.

Melania Olivia SANDU, PhD Candidate, Politehnica University of Timișoara, Department of Mechatronics, melania.sandu@upt.ro, +40256403551, Mihai Viteazul Bd., no. 12, Timișoara.

Erwin-Christian LOVASZ, Dr. ing., Head of Mechatronics Department, Professor, Politehnica University of Timișoara, Department of Mechatronics, erwin.lovasz@upt.ro, +40256403569, Mihai Viteazul Bd., no. 12, Timișoara.